Twisted-chiral mesoporous silica from coconut husk waste designed for high-performance drug uptake and sustained release

by Ery S. Retnoningtyas

Submission date: 12-Feb-2025 04:29AM (UTC+0700)
Submission ID: 2586027179
File name: 7-Twiste-chiral_mesoporous_silica_from.pdf (3.48M)
Word count: 8014
Character count: 42056

Microporous and Mesoporous Materials 367 (2024) 112973

Contents lists available at ScienceDirect

Microporous and Mesoporous Materials

journal homepage: www.elsevier.com/locate/micromeso

Twisted-chiral mesoporous silica from coconut husk waste designed for high-performance drug uptake and sustained release

Jeane Angelica Yulianadi Susanto [a,b], Antonius Jimmy Widagdo [a,b], Marvel Guntur Wijanarko [a,b], Maria Yuliana [a,b,c,*], Sandy Budi Hartono [a,c], Shella Permatasari Santoso [a,b,c], Grandprix Thomryes Marth Kadja [d,e,f], Christian Julius Wijaya [a,c], Aning Ayucitra [a,b], Ery Susiany Retnoningtyas [a,b], Hidayat [c,g], Suryadi Ismadji [a,c]

[a] Department of Chemical Engineering, Widya Mandala Surabaya Catholic University, Kalijudan 37, Surabaya, 60114, Indonesia
[b] Chemical Engineering Master Program, Widya Mandala Surabaya Catholic University, Kalijudan 37, Surabaya, 60114, Indonesia
[c] Collaborative Research Center for Zero Waste and Sustainability, Kalijudan 37, Surabaya, 60114, Indonesia
[d] Division of Inorganic and Physical Chemistry, Faculty of Mathematics and Natural Sciences, Institut Teknologi Bandung, Ganesha 10, Bandung, 40132, Indonesia
[e] Center for Catalysis and Reaction Engineering, Institut Teknologi Bandung, Ganesha 10, Bandung, 40132, Indonesia
[f] Research Center for Nanosciences and Nanotechnology, Institut Teknologi Bandung, Ganesha 10, Bandung, 40132, Indonesia
[g] Research Center for Environmental and Clean Technology, National Research and Innovation Agency, Kawasan Puspiptek Gedung 820, Tangerang Selatan, 15314, Indonesia

ARTICLE INFO

Keywords:
Biomass-based silica
Twisted-chiral structure
Sustainable material
Mesoporous material
Tetracycline
Drug uptake/release

ABSTRACT

With an annual production of 2.81 million tons, the coconut husk is an essential source of silica. Various advantages of silica as a drug carrier make it one of the most developed materials in drug delivery applications. To improve the drug delivery performance of a material, twisted chirality is also classified as a critical factor because the pharmacological activity depends on the interaction of the drug with the drug carrier material in the target area. In this study, the coconut husk-based mesoporous silica (MS) can be synthesized through a calcination and sol-gel method. With the help of anionic surfactant, MS is successfully modified to have a twisted-chiral structure (CMS). CMS is characterized by twisted rod-like morphology at a size of 1–2 μm, with a helical arrangement (mixed with the beta-sheet and random coil conformations). CMS's surface area and pore volume are obtained at 288.3 m^2/g and 0.614 cm^3/g, with an average pore size of 7.63 nm. The maximum adsorption of tetracycline (506.5 mg/g) is reached at pH = 4, with the initial concentration of tetracycline at 400 mg/g, temperature of 323 K, and adsorption time of 600 min. The loading of tetracycline follows the pseudo-first-order model with a monolayer mechanism. The bulk migration of tetracycline from the solution into the surface of CMS is deemed the primary adsorption mechanism. The in-vitro release study of tetracycline at pH = 7.4 follows the slow-sustained release model with the cumulative release at 72.3 %, showing better release performance compared with the common MS.

1. Introduction

Silica, in the form of mesoporous silica (MS), finds uses in many applications, including pharmaceutical and drug delivery [1], due to the ease of synthesis and surface modification, large surface area, tunable pore size, biocompatibility, and bioavailability properties [2]. The highly ordered molecule structure owned by MS might also increase drug loading, reduce rapid drug release, and prevent physical particle degradation [3–5]; hence, suitable for the delivery of various drug molecules, proteins, peptides, and genes [6–8]. Recently, a site-specific drug delivery system (DDS) has become an essential route to direct and deliver drugs to the target site, improving treatment outcomes. This type of DDS can be achieved by loading the medicine into a suitable nanoporous carrier that can actively approach the target site. Most drugs and their biological targets are twisted-chiral, meaning the drug carrier must also be of a twisted structure to host and deliver the drug to the target

* Corresponding author. Department of Chemical Engineering, Widya Mandala Surabaya Catholic University, Kalijudan 37, Surabaya, 60114, Indonesia.
E-mail address: mariayuliana@ukwms.ac.id (M. Yuliana).

https://doi.org/10.1016/j.micromeso.2023.112973
Received 22 October 2023; Received in revised form 13 December 2023; Accepted 29 December 2023
Available online 3 January 2024

adequately. Current research has proved that twisted chirality promotes better drug delivery and is a critical factor in drug development. Fan et al. (2019) and Gou et al. (2022) reported that combining carrier material and twisted-chiral structure may increase the chiral recognition of the drug to both carrier and biological target, indicated by specific responses, e.g., high drug adsorption, targeted distribution, quick pharmacodynamics metabolism, transmembrane, and protein increase [9,10]. Another study by Hu and Wang (2020) specifically mentioned that integrating chirality into MS forms a crimp/twisted channel within the structure, further stimulating drug absorptivity and resulting in more effective drug loading than common MS [11].

This study utilizes coconut husk waste (CHW) as the silica source, replacing the commonly employed synthetic silica precursors, e.g., tetraethyl orthosilicate (TEOS), tetramethyl orthosilicate (TMOS), and others. In Indonesia, coconut husk waste (CHW) accumulated about 2.81 million tons in 2020 with minimum effort to use in practical application. Coconut husk contains various components, e.g., cellulose, lignin, hemicellulose, and ash, with silica as the most prominent compound, which accounts for 35 % of coconut husk ash [12,13]. This leaves 39,340 tons of silica remaining in CHW, rendering an abundant material to fabricate valuable material such as twisted-chiral mesoporous silica (CMS). Several studies have been employed to produce MS from natural biomasses using the following routes: (1) microemulsion technique, sonochemical synthesis, acid leaching, alkaline treatment, and sol-gel method [14–16]. Of the available courses, the sol-gel process is the most efficient technique, facilitating surface modification and providing high stability and surface area [17].

Several template molecules to imprint the chiral structure into MS include amino acids (i.e., DOPA, tyrosine), sugar, organogel, nanometals, propranolol, and surfactants [18,19]. Various surfactants, such as anionic, cationic, and non-ionic, can be used as twisted-chiral templates. However, anionic surfactant offers some advantages owing to its non-toxicity and bio-mimic function to distribute drug molecules into animal lungs and brains [10,20]. Several anionic chiral surfactants with twisted forms can be made by chiral amino acid combined with co-structure directing agents such as 3-aminopropyl-triethoxysilane (APTES), $_{N}$-trimethoxysilylpropyl-$_{N}$, $_{N}$, $_{N}$-trimethylammonium chloride (TMAPS), 3-aminopropyltrimethoxysilane (APS) [21]. $_{L}$-arginine/$_{N}$-miristoyl-$_{L}$-alanine (C_{14}-L-AlaA), $_{N}$-myristoyl-$_{L}$-alanine sodium salt (C_{14}-L-AlaS), cetyltrimethylammonium bromide (CTAB), and $_{N}$-palmitoyl-$_{DL}$-glutamic acid are some types of anionic surfactants that are used as twisted-chiral template with final morphology as a twist-rod like [22]. Among the available surfactants, this study selects $_{N}$-palmitoyl-$_{DL}$-glutamic acid as an anionic surfactant for the twisted-chiral template of MS. $_{N}$-palmitoyl-$_{DL}$-glutamic acid shows superiority because of its high selectivity, low toxicity, stability, biodegradability, and versatility. This component finds applications in various fields, e.g., chromatography, drug delivery, and microemulsions [23]. Gayathiri et al. (2022) also reported that $_{N}$-palmitoyl-$_{DL}$-glutamic acid has low toxicity because it is considered a natural amino acid safe for pharmaceutical applications [24]. Further, $_{N}$-palmitoyl-$_{DL}$-glutamic acid shows good stability in a wide pH range and temperature and is biodegradable, which means it can degrade naturally over time in the environment compared to the other surfactants.

This study uses tetracycline as the drug model to test the obtained twisted-chiral MS (CMS) performance. Tetracycline is mainly applied to manage and treat various bacterial infections and works by blocking the bond of 30S ribosome and aminoacyl-tRNA from the acceptor, which promotes the bacteriostatic condition – in this condition, bacteria cannot functionalize, grow, and replicate [25]. Often prescribed as long-term medicine for local wounds, tetracycline may cause various side effects and multi-drug resistance (MDR) [26,27]; therefore, loading the drug to the suitable carrier will limit the usage frequency, improve selectivity and safety of drug administration [28,29]. Several MS-based materials have been reported to deliver tetracycline – Das et al. (2012) present that the hollow sphere mesoporous phosphosilicate nanoparticles are efficient in encapsulating tetracycline, particularly due to the presence of the hollow core and phosphonium cations in the materials. This work observes the controlled release of the tetracycline molecules in an aqueous medium with the presence of various bio-relevant metal ions [30]. A similar result is seen in the study conducted by Lin et al. (2009), which mentions that the hollow (empty) core in their periodic mesoporous organosilica may act as the reservoir to encapsulate and store a larger amount of tetracycline and at the same time, decline the release rate of the drug [31].

Looking at the suitability of MS-based materials and how the interior structures of a material affect drug delivery, our key focuses in this study are (1) to observe the potential utilization of CHW in synthesizing a drug carrier, (2) to imprint twisted-chiral structures in MS using an anionic chiral surfactant, and (3) to evaluate its performance in the tetracycline uptake/release. The uptake performance is conducted in various pH and initial concentrations (C_o) and further illustrated using kinetic, isotherm, and thermodynamic studies. The in-vitro release profile of tetracycline from CMS is also investigated at pH 7.4.

2. Material and methods

2.1. Material

CHW is obtained from a local supplier in Bandung, Indonesia. Sulfuric acid (H_2SO_4, CAS#7664-93-9, ≥98 % purity), $_{DL}$-glutamic acid monohydrate (CAS#19285-83-7, ≥98 % purity), palmitoyl chloride (CAS#112-67-4, ≥97.5 % purity), and acetone (CAS#67-64-1, ≥99 % purity) are purchased from Sigma Aldrich (Germany), while sodium hydroxide (NaOH, CAS#1310-73-2) is procured from Merck (Germany). All chemicals are of reagent grade and used without purification.

2.2. Fabrication of CMS

In a typical purification of silica, the coconut husk is initially calcined at 650 °C for 2 h to produce ashes. Approximately 4.5 g of coconut husk ash are dispersed with 100 mL NaOH solution (10 wt% in water) and stirred for 1 h at 80 °C. After the reaction, the solid is filtered, while the supernatant is cooled down and titrated with H_2SO_4 5 N solution until the pH reaches 7, at which the silica gels are formed. The silica gels are repeatedly washed with distilled water and oven-dried at 100 °C. The obtained silica powders are subjected to a refluxed reaction system with NaOH solution for 24 h to obtain the sodium silicate solution.

The twisted-chiral imprinting is conducted by typical hydrolysis and condensation reactions of silica over the chiral surfactant. The chiral anionic surfactant ($_{N}$-palmitoyl-$_{DL}$-glutamic acid) with twisted structures is prepared using a method by Takehara et al. (1972) [32]. At room temperature, a certain amount of anionic surfactant (0.54 g) is diluted into 37 mL sodium silicate for 6 h. The solution will be then adjusted to pH = 11 and aged at 100 °C for 36 h to obtain CMS. The aged CMS is calcined at 650 °C for 10 h to remove the remaining surfactant.

2.3. Characterization of CMS

The crystal structure of coconut husk based-MS is analyzed by X-ray Diffraction (XRD) analysis using the X'PERT Panalytical Pro X-Ray diffractometer (Philip-FEI, Netherland) at 2θ = 5–60°, tube current = 20 mA, running voltage = 40 kV, and constant Cu $K_{\alpha 1}$ radiation (λ = 1.5406 Å). Meanwhile, its mesopore nanostructure is observed on a Malvern PANalytical Empyrean (Malvern Panalytical, United Kingdom) small-angle X-ray scattering (SAXS) with a Cu-K_{α} X-ray tube, at 2θ = 1–5°. The microscopic feature of CMS is captured using a JEOL JSM-6500F (Jeol Ltd., Japan) at an accelerating voltage of 300 kV and a working distance of 0.6 mm. The chirality structure of CMS is investigated using a Jasco J-1500 circular dichroism (CD) spectrophotometer (Jasco Inc., Canada). To measure the textural properties of CMS, the N_2

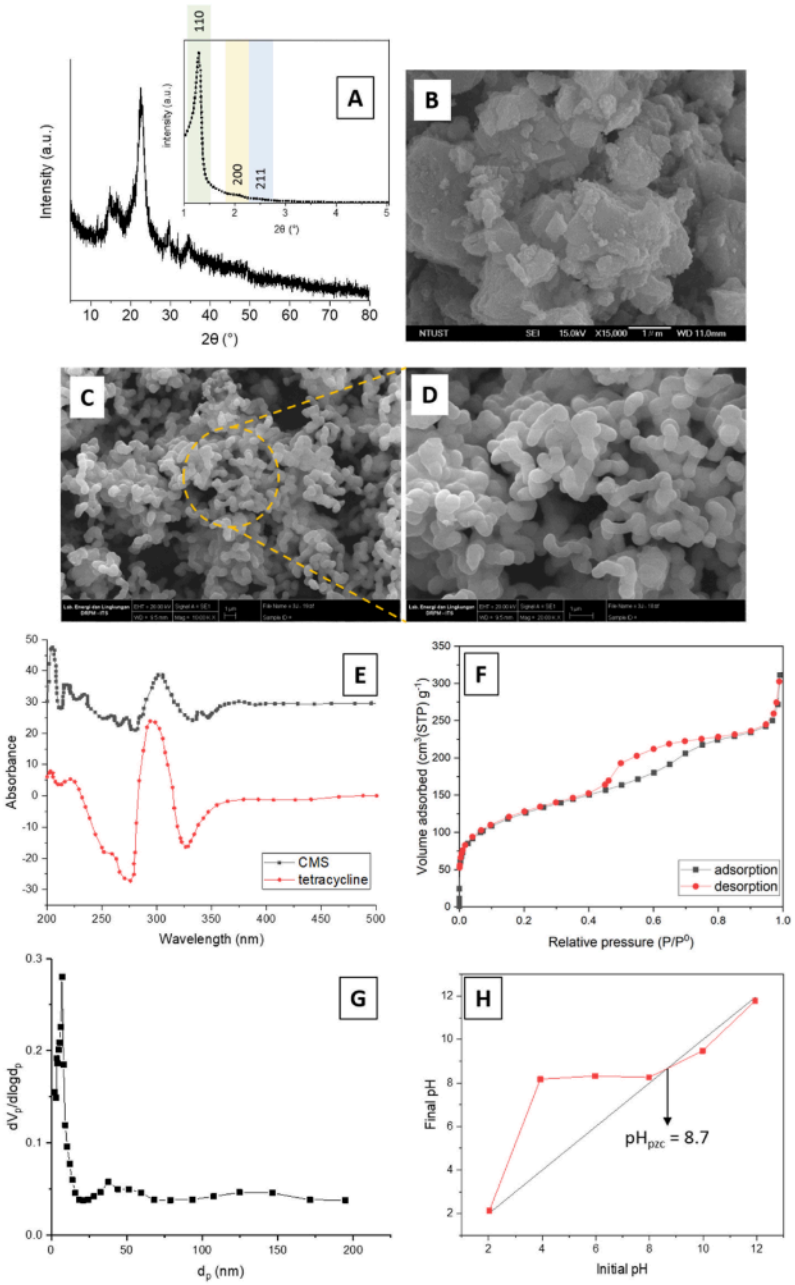

Fig. 1. A. The XRD pattern of CMS, and (inset) its SAXS analysis; B. SEM of CHW-based silica; C-D. SEM of CMS; E. CD spectra of CMS, F. N_2 Sorption profile of CMS; G. BJH pore distribution plot of CMS; H. pH_{pzc} of CMS.

sorption analysis is carried out at 77 K using a micromeritics ASAP 2010 sorption analyzer (Micromeritics Instrument Corporation, USA) after degassing the sample for 2 h at 423 K. The point-of-zero-charge (pH_{pzc}) of CMS is measured using the drift method with a pH range of 2–12.

2.4. Uptake study of tetracycline into CMS

To study the performance of CMS in the tetracycline uptake, CMS with the adsorbent loading, m_a = 0.03 wt% is introduced to the tetracycline solution at various pH (pH = 2, 4, 6, 8, 10, 12) and initial drug concentrations (C_o = 100, 200, 300, 400, 500 mg/L); each batch is collected after a 12-h stirring at 30 °C to determine the loaded tetracycline amount in CMS. The pH and initial drug concentration giving the highest uptake of tetracycline (pH_{opt} and C_{oopt}) are employed throughout the kinetic and isotherm studies.

The kinetic study is conducted by mixing 0.03 wt% CMS into a series of tetracycline solution flasks. The adsorption duration and temperature are varied at t = 10–600 min and T = 303–323 K. All experiments are

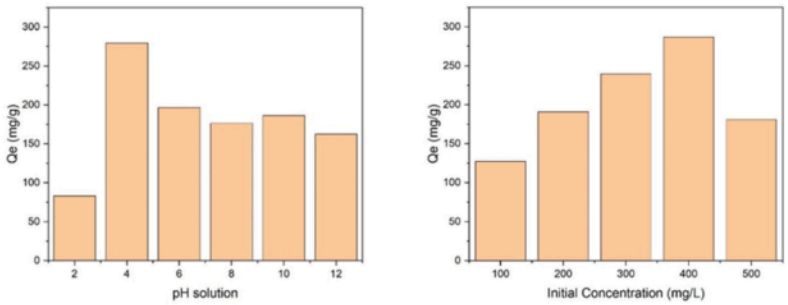

Fig. 2. The influence of the pH (left), and initial concentration (right) for tetracycline adsorption.

carried out using 400 mg/L of tetracycline solution (400 mg/L in ethanol). Meanwhile, the isotherm study uses various CMS loading on the adsorption system (C_o = 100, 200, 300, 400, 500, 600, 700 mg/L) with an adsorption time of t = 600 min. Similarly, three levels of temperature are also employed for this study. The remaining tetracycline amount in the supernatant is measured by Shimadzu UV–Vis spectrophotometer 2600 (Shimadzu, Japan) at a wavelength (λ) of 277 nm. The amount of tetracycline adsorbed into CMS at a particular time (t) and equilibrium (t_{eq}) can be computed using equations (1) and (2).

$$Q_t\ (mg/g) = \frac{V(C_o - C_t)}{m_s} \quad (1)$$

$$Q_e (mg/g) = \frac{V(C_o - C_e)}{m_s} \quad (2)$$

Where C_o (mg/L) is the initial concentration of tetracycline in solution, C_t (mg/L) is the concentration of tetracycline at a particular time, C_e (mg/L) is the concentration of tetracycline at equilibrium conditions, V (L) is the volume of the tetracycline solution, m_s (g) is the mass of CMS used in an adsorption batch. Both kinetic and isotherm data are then fitted to several adsorption models to elucidate the adsorption behavior. The employed adsorption models and parameters are summarized in Table S1. Further, the obtained isotherm parameters are used to calculate the thermodynamic properties – Gibbs free energy ($\Delta G°$), enthalpy ($\Delta H°$), and entropy ($\Delta S°$).

2.5. In-vitro release study

The in-vitro release is carried out by dispersing 3 mg tetracycline-loaded CMS (Te@CMS) into 5 ml phosphate buffer solution (PBS) placed in the dialysis membrane. Subsequently, the membrane containing the mixture is immersed in a more extensive 500 ml PBS solution; the system is slow-stirred at 37 °C. A 5-ml solution is taken at different release times, membrane-filtered, and analyzed using Shimadzu UV–Vis spectrophotometer 2600 (Shimadzu, Japan) at λ = 270 nm. Simultaneously, a new PBS solution with the same volume is added to maintain the volume of the release system. The release system is set to pH = 7.4 to mimic the human body fluid. In this study, the release profile of pure tetracycline and tetracycline-loaded MS are also observed for comparison.

3. Result and discussion

3.1. Characteristics of CMS

The CHW-based twisted-chiral mesoporous silica (CMS) particles are successfully synthesized by sol-gel method on the twisted-chiral templated surfactant, followed by calcination at 650 °C to eliminate the template. The XRD pattern (Fig. 1A) confirms the amorphous phase of SiO_2 at 2θ = 22.3, within the range between 2θ = 20–25° as reported by Huo et al. (2015) and Mohamed et al. (2017) [33,34]. The SAXS analysis (Fig. 1A (inset)) exhibits three well-defined peaks for 110, 200, and 211 planes, with their respective d_{hkl} of 7.40, 6.10 and 4.60 nm. This result suggests the existence of mesostructured spacings in the CMS particles.

The morphology structures of CHW-based silica and its derived CMS can be seen in Fig. 1B–D. The waste-derived silica particles (Fig. 1B) are irregular in shape with a size range of 600 nm–2 μm. Meanwhile, Fig. 1C–D shows that CMS has a twisted rod-like form, indicating that the twisted chirality has been successfully incorporated into the MS particles using $_N$-palmitoyl-$_{DL}$-glutamic acid as a template; the average particle size of CMS is 1–2 μm. The CD analysis is also introduced to check the chirality of CMS using the tetracycline as the chiral probe. As displayed in Fig. 1E, the CD spectra of both the tetracycline probe and CMS share a similar profile, with non-zero signals located in the range of 205–210 nm, 220–225 nm, 260–265 nm, and 295–300 nm. These non-zero spectra exhibit the chirality of CMS, with the helical arrangement of electrons during electronic transitions. Similar to the study conducted by Surma et al. (2014), a further observation of the spectra also shows that the CMS does not consist of only the α-helix fraction, but there is a combination of β-sheet and random coil conformation as well [35]. A CDSSTR algorithm is, however, required to confirm the result.

N_2 sorption analysis is performed to measure the porosity of CMS. The surface area (S_{BET}), and pore volume (V_p) of CMS are obtained at 288.3 m^2/g and 0.614 cm^3/g, respectively. Fig. 1F shows hysteresis loop IUPAC type IV, indicating the presence of mesopores. This result is verified by the Barrett-Joyner-Halenda (BJH) analysis (Fig. 1G) where the highest pore distribution of CMS is found in the range of pore diameter (d_p) = 2.43–9.26 nm, with the average pore width at 7.63 nm. The adsorption profile shows an unrestricted monolayer to multilayer adsorption up to high $P/P°$. Meanwhile, the desorption profile reveals a small bottleneck bump in the $P/P°$ range of 0.5–0.8, showing a small resistance from the pore shape. The graph presents a sharp increase nearing $P/P° = 1.0$, implying the completion of monolayer coverage. However, it cannot be directly assumed as a monolayer mechanism due to the possibility of monolayer-multilayer adsorption, as this type of hysteresis loop can also occur by a pore not filled with condensate due to non-rigid aggregated rod-like materials [36]. Therefore, kinetic and isotherm studies are also required to illustrate the adsorption behavior. The pH_{pzc} of CMS is found at pH = 8.7; the profile is shown in Fig. 1H. This explains that at pH < 8.7, the particle of CMS will be protonated and has a positive ion charge; at pH > 8.7, the material will be in an anionic form and have a negative ion charge [37].

3.2. Drug loading study

3.2.1. Influence of pH and initial concentration of tetracycline

The influence of pH is studied by adjusting the pH of tetracycline from 2 to 12 using 0.1 M NaOH solution and 0.1 M HCl solution. The result shows that the maximum uptake of tetracycline occurs at pH 4. According to Li et al. (2010) and Manzar et al. (2023), the maximum

Table 1
Kinetic parameters of tetracycline adsorption into CMS.

Parameters	Temperature (K)		
	303	313	323
PFO			
Q_e (mg/g)	336.1	358.4	411.3
k_1 (1/min))	0.006	0.011	0.014
R^2	0.9963	0.9905	0.9904
PSO			
Q_e (mg/g)	439.7	434.8	477.7
k_2 (g/(mg min))	1.29×10^{-5}	2.36×10^{-5}	3.30×10^{-5}
R^2	0.9941	0.9945	0.9815
IPD			
k_{IPD} (mg/(g.min$^{1/2}$))	14.67	16.23	17.85
$k_{IPD\ 1}$	1.769	2.625	4.203
$k_{IPD\ 2}$	0.822	0.689	0.685
$k_{IPD\ 3}$	0.089	0.167	0.065
C	9.99×10^{-27}	20.07	53.42
R^2	0.9692	0.9531	0.8699

adsorption of tetracycline occurs in acidic conditions and will decrease with the increase in pH [38,39]. In addition, the pH_{PZC} value for CMS is at pH = 8.7, and according to the result seen in Fig. 2 (left), the CMS particle will have a positive charge below pH 8.7 and a negative charge at pH > 8.7. As reported by Jang and Kan (2019) and Wang et al. (2008), the pK_a value of tetracycline is located at 3.57, 7.49, and 9.88, and can be divided into cationic (at pH < 3.57), zwitterionic (at pH = 3.57–7.49), and anionic (at pH > 7.49) predominant species [37,40]. Adsorption of tetracycline in the zwitterion phase works along with proton saturation, which will increase tetracycline affinity on the surface of CMS [41]. On pH > 6, the CMS surface has a negative charge, and tetracycline is in the anionic phase. Moreover, tetracycline tends to hydrophobically interact with each other at basic conditions and form large aggregates that are unable to be absorbed into the CMS pore [42]. Therefore, the adsorption of tetracycline at pH > 6 is lower than its performance at pH = 4. Although not as strong, it can be seen that quite a substantial amount of tetracycline can still be uptaken by CMS at pH > 6; this is likely due to the deposition of the tetracycline aggregates on the undissociated silanol group of silica, which reduces the repulsive force between tetracycline and CMS.

Initial concentration is studied by adjusting the concentration of tetracycline from 100 to 500 mg/L and pH 4. The result shows that the maximum adsorption of tetracycline occurred when the initial concentration was 400 mg/L (Fig. 2 (right)). The increase in tetracycline concentration will cause higher adsorption of tetracycline due to the rise of tetracycline mass transfer from the bulk solution to the CMS surface [43,44]. However, escalating the initial concentration higher than 400 mg/L turns out declines the adsorption capacity of tetracycline onto CMS; perhaps, due to the aggregation of tetracycline at higher concentration.

3.2.2. Kinetic adsorption study

Tetracycline loading is studied at various times and temperatures with C_o = 400 mg/L. The adsorption rate is fast until 120 min, then reach its equilibrium state from 240 min to 600 min. The kinetic adsorption is fitted into some kinetic models, such as pseudo-first-order (PFO), pseudo-second-order (PSO), and intraparticle diffusion (IPD). The overall result, as mentioned in Table 1, shows that all R^2 values are close to unity in all temperatures, which suggests that both PFO and PSO can describe the adsorption process of tetracycline into CMS. However, from Fig. 3, all data can be concluded is more fitted in PFO based on the Q_e value approach, which implies that the adsorption is controlled by physisorption. The k_1 value that rises with the increasing temperature shows that the adsorption is endothermic in which adsorption capacity will increase as the temperature increases [45]. The activation energy is also obtained at 32.682 kJ/mol (see Fig. 4).

The IPD model is conducted to study the migration of tetracycline from the bulk solution into the CMS. There are 3 stages of adsorption based on the IPD result: surface diffusion, intraparticle diffusion, and adsorption-desorption equilibrium [46]. At first, the tetracycline will be transferred from bulk solution into the CMS surface, then continue with slow diffusion of tetracycline from the boundaries layer into pores of CMS, and finally, the chemical binding of tetracycline into active sites of

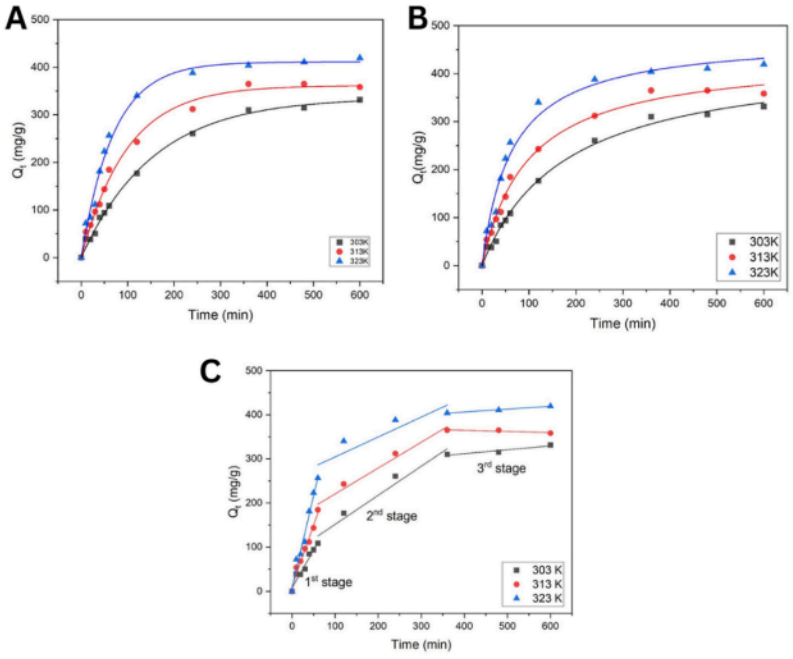

Fig. 3. The kinetic study of tetracycline adsorption into CMS – A. PFO, B. PSO, C. IPD (C_o = 400 mg/L, m_a = 0.03 wt%, pH = 4.0).

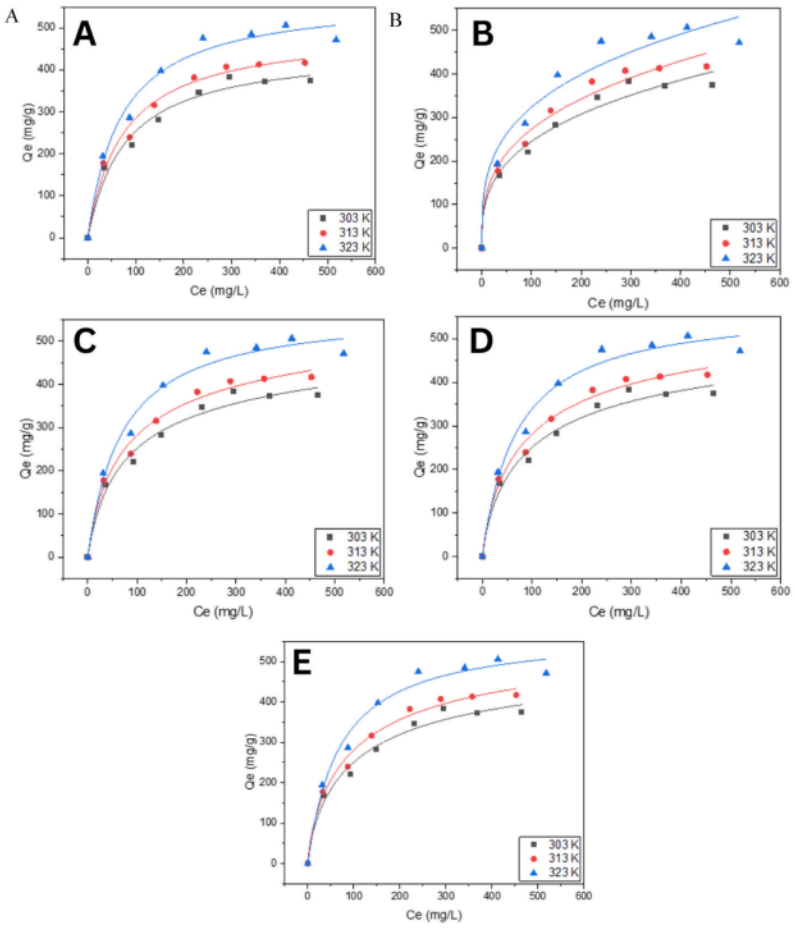

Fig. 4. The equilibrium data fitted to various isotherm models (A. Langmuir, B. Freundlich, C. Redlich-Peterson, D. Toth, E. Sips).

Table 2
Isotherm parameter of tetracycline adsorption into CMS.

Parameter	Temperature (K)		
	303	313	323
Langmuir			
$Q_{m(L)}$ (mg/g)	451.6	495.5	573.6
k_L (L/mg)	0.013	0.014	0.015
R^2	0.9813	0.9875	0.9807
Freundlich			
k_F ((mg/g)(L/mg)$^{1/n}$)	54.31	60.58	80.95
$1/n_F$	0.331	0.327	0.301
R^2	0.9756	0.9811	0.9579
Redlich-Peterson			
k_{RP} (L/mg)	7.67	8.83	8.31
α_{RP} (L/mg)^g	0.022	0.023	0.015
G	0.896	0.898	1.000
R^2	0.9823	0.9886	0.9834
Toth			
$Q_{m(t)}$ (mg/g)	579.9	606.1	573.6
k_t ((mg/L)^{nt})	11.53	12.35	69.02
n_t	0.613	0.643	1.000
R^2	0.9806	0.9895	0.9834
Sips			
$Q_{m(S)}$ (mg/g)	530.7	576.0	568.7
k_s ((L/mg)^{ns})	0.032	0.028	0.013
n_s	1.356	1.303	1.000
R^2	0.9781	0.9899	0.9834

CMS. According to the k_{IPD} value that can be seen in Table 1, k_{IPD1} is larger than the other k_{IPD} in each temperature level, which means the diffusion of tetracycline from bulk solution into CMS surface is the main parameter in the adsorption and followed by intraparticle diffusion and physical binding of tetracycline into active sites of CMS. Table 1 also shows an increasing value of the surface adsorption constant (C) along with temperature. The C constant is proportional to (1) the thickness of the boundary layer on the surface of CMS, and (2) the viscous drag between the surface of CMS and the tetracycline solution caused by the presence of the boundary layer [47,48]. From the thermodynamic viewpoint, this viscous drag will enhance the entropy of the system – creating a more intensive random movement of the molecules which triggers a greater adsorption capacity. Therefore, the escalating profile of C suggests that there is a larger contribution of surface binding during the uptake process [48,49] at higher temperatures which leads to better uptake of tetracycline. This phenomenon confirms the endothermic nature of the tetracycline adsorption into CMS.

3.2.3. Isotherm and thermodynamic adsorption study

Isotherm study has been conducted using Langmuir, Freundlich, Redlich-Peterson, Toth, and Sips models; the summarized data can be seen in Table 2. The study shows that the highest uptake of tetracycline using CMS is obtained at 506.5 mg/g at the following adsorption conditions: pH = 4, C_o = 400 mg/L, T = 323 K, and t = 600 min – higher

Table 3
Thermodynamic parameters of tetracycline adsorption into CMS.

Temperature (K)	ΔG° (kJ/mol)	ΔH° (kJ/mol)	ΔS° (J/mol.K)
303	−1.353	14.77	53.20
313	−1.885		
323	−2.417		

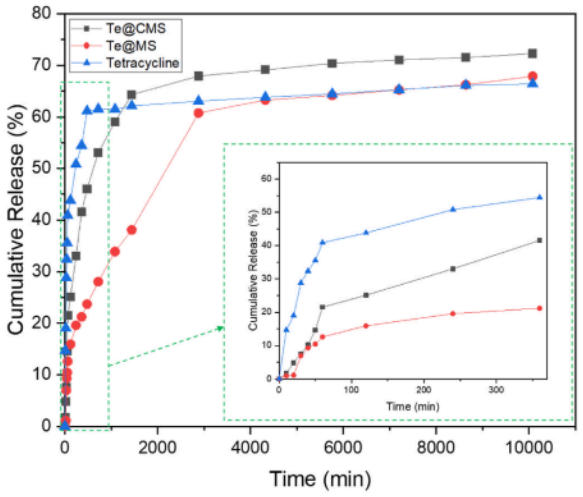

Fig. 5. The in-vitro release study of pure tetracycline, Te@MS, and Te@CMS

than that reported in previous studies. Hanh et al. (2023) reported that bottom ash-based magnetic mesoporous silica has an adsorption capacity of tetracycline at 276.74 mg/g [50], while Brigante and Avena (2016) studied that MS templated by the biopolymer hydroethyl starch may uptake tetracycline until 20 μmol/g (about 8.9 mg/g) [51]. This result shows that CMS exhibits a high affinity towards tetracycline, which is likely because both materials have chirality in their molecule structures.

According to Fig. 3, the L-curve shape follows Giles classification with subclass 2, which implies the adsorption of tetracycline continuously increases linearly as the initial concentration until the binding sites of the particle reach their saturation capacity [52]. Therefore, there is no competition in the adsorption of tetracycline into the CMS surface or between solvent and adsorbate attached at the binding sites [53]. The R^2 value of the Langmuir method that can be seen in Table 2 is more fitted than Freundlich, which indicates the adsorption of tetracycline into CMS follows the monolayer mechanism. It also implies that the surface of CMS is homogeneous [54,55]. Moreover, it is also confirmed by the three other methods, which are Redlich-Peterson, Toth, and Sips model, where the α_{RP}, n_t, dan n_s values are increasing toward 1 with $R^2 > 0.98$ in every temperature level that indicates the adsorption is homogenous [56]. The increasing adsorption capacity ($q_{m(L)}$ = 451.6–573.6 mg/g) as the temperature increases (T = 303–323K) also confirms the endothermic reaction. The thermodynamic study is conducted using Gibbs free energy changes (ΔG°), enthalpy (ΔH°), and entropy (ΔS°); the results can be seen in Table 3. The adsorption of tetracycline into CMS is spontaneous and favorable, as confirmed by the negative value of ΔG°. The endothermic reaction also can be approved by the positive ΔH° and the positive ΔS° value indicating the randomness of adsorbate-solution during adsorption increase [57].

3.3. Drug release study

A drug release study is conducted at pH = 7.4 for 7 days at 37 °C.

Table 4
The first-order kinetic parameters for tetracycline release.

Parameter	Te@CMS	Te@MS	Tetracycline
k (min^{-1})	0.003	0.001	0.015
m_o (mg)	78.51	65.39	58.63
R^2	0.9730	0.9545	0.9255

Fig. 5 reveals that the release of tetracycline from pure tetracycline, tetracycline loaded in MS (Te@MS), and Te@CMS follows the slow-sustained first-order profile [58]. The release data are then fitted to the model, and the obtained parameters are summarized in Table 4. As seen, the coefficients of determination (R^2) for all materials are close to unity, implying the suitability of the first-order model to the release data. The initial loaded amount of tetracycline (m_o) in Te@CMS is also found to be higher than that of Te@MS – which verifies the ability of CMS to load tetracycline in greater amounts as compared with the common MS. Meanwhile, the release rates of tetracycline from Te@MS (k = 0.001/min) and Te@CMS (k = 0.003/min) are much lower than that of pure tetracycline (k = 0.015/min), indicating that loading tetracycline to a drug carrier may prevent the burst release.

As seen in Fig. 5, the release of tetracycline from Te@CMS reaches equilibrium after a week, with a cumulative release of 72.3 %, while the cumulative releases of pure tetracycline and tetracycline loaded in MS (Te@MS) reach only 66.4 % and 69.1 %, respectively. Fig. 5 (inset) shows that in the first hour, about 41 % of pure tetracycline has already been released, while only 13.9 % and 21.5 % of tetracycline are cumulatively released from Te@MS and Te@CMS – indicating the burst release characteristics of pure tetracycline. In this early stage, Te@MS shows a slower release compared to Te@CMS. However, during the second stage, a sharp rise in the cumulative release is monitored in Te@MS, while Te@CMS maintains its consistency in sustaining a slow release of the drugs, which is expected due to the twisted pore channels CMS possesses. This phenomenon proves that CMS has a better release profile. The results of this sustained release of tetracycline from CMS can be the answer to cope with the possibility of multi-drug resistance, as it can provide a stable therapeutic effect for certain patients required to take antibiotics for a longer time.

4. Conclusions

CMS is successfully fabricated using the sol-gel method with a particle size of 1–2 μm from SEM analysis, a surface area of around 288.3 m^2/g, a pore volume of 0.614 cm^3/g, and an average mesopore size of 7.63 nm. The twisted chirality is successfully impregnated in the helical arrangement (mixed with beta-sheet and random coil conformations), as confirmed by the CD analysis. With the pH_{PZC} at pH = 8.7, the CMS can adsorb tetracycline very well in acidic conditions, and the highest adsorption occurs at pH = 4 with an initial concentration of C_o = 400 mg/g. The kinetic adsorption study shows that the adsorption data can be fitted to both PFO and PSO; however, according to the Q_e value, the adsorption process is more likely to follow PFO, which indicates that the adsorption process is driven by physisorption. The intraparticle diffusion study confirms that the main driving force in the adsorption is when the tetracycline molecule diffuses into the surface of CMS. In the isotherm study, the Langmuir model is more suitable for illustrating adsorption behavior, where the adsorption follows the monolayer mechanism. The adsorption of tetracycline into CMS occurs in a spontaneous and endothermic nature. The release study shows that CMS slowly releases the tetracycline, and the sustained release process is in equilibrium after a week with a cumulative percentage release of 72.3 %. The profile of the release study follows the first-order release model, which shows that the amount of tetracycline released in the PBS solution is proportional to the amount of remaining tetracycline in CMS. This work concludes that the twisted morphology of CMS causes the material to slowly release the antibiotic so that the same dosage may be delivered

longer without causing any side effects like multi-drug resistance.

CRediT authorship contribution statement

Jeane Angelica Yulianadi Susanto: Writing – original draft, Visualization, Software, Methodology, Investigation, Conceptualization. **Antonius Jimmy Widagdo:** Software, Methodology, Investigation. **Marvel Guntur Wijanarko:** Software, Methodology, Investigation. **Maria Yuliana:** Writing – review & editing, Supervision, Resources, Project administration, Methodology, Funding acquisition, Conceptualization. **Sandy Budi Hartono:** Supervision, Resources, Methodology, Funding acquisition, Data curation. **Shella Permatasari Santoso:** Visualization, Validation, Software. **Grandprix Thomryes Marth Kadja:** Visualization, Software, Investigation. **Christian Julius Wijaya:** Validation. **Aning Ayucitra:** Validation. **Ery Susiany Retnoningtyas:** Validation. **Hidayat:** Software, Investigation. **Suryadi Ismadji:** Resources, Funding acquisition, Data curation.

Declaration of competing interest

The authors declare that they have no known competing financial interests or personal relationships that could have appeared to influence the work reported in this paper.

Data availability

Data will be made available on request.

Acknowledgment

The authors thank the Institut Teknologi Bandung for providing the facilities for material characterizations. This project was supported by the Ministry of Education, Culture, Research, and Technology of the Republic of Indonesia and Widya Mandala Surabaya Catholic University through research grant no. 260C/WM01.5/N/2023, 268G/WM01.5/N/2023, and 7405/WM01/N/2022.

Appendix A. Supplementary data

Supplementary data to this article can be found online at https://doi.org/10.1016/j.micromeso.2023.112973.

References

[1] S. Steven, E. Restiawaty, Y. Bindar, Routes for energy and bio-silica production from rice husk: a comprehensive review and emerging prospect, Renew. Sustain. Energy Rev. 149 (2021), https://doi.org/10.1016/J.RSER.2021.111329.
[2] A. Bernardos, E. Piacenza, F. Sancenón, M. Hamidi, A. Maleki, R.J. Turner, R. Martínez-Máñez, Mesoporous silica-based materials with Bactericidal properties, Small 15 (2019) 1–34, https://doi.org/10.1002/smll.201900669.
[3] Y. He, S. Liang, M. Long, H. Xu, Mesoporous silica nanoparticles as potential carriers for enhanced drug solubility of paclitaxel, Mater. Sci. Eng. C 78 (2017) 12–17, https://doi.org/10.1016/J.MSEC.2017.04.049.
[4] S. Jafari, H. Derakhshankhah, L. Alaei, A. Fattahi, B.S. Varnamkhasti, A. A. Saboury, Mesoporous silica nanoparticles for therapeutic/diagnostic applications, Biomed. Pharmacother. 109 (2019) 1100–1111, https://doi.org/10.1016/j.biopha.2018.10.167.
[5] K.-C. Kao, C.-Y. Mou, Pore-expanded mesoporous silica nanoparticles with alkanes/ethanol as pore expanding agent, Microporous Mesoporous Mater. 169 (2013) 7–15, https://doi.org/10.1016/j.micromeso.2012.09.030.
[6] C.Z. Xu, G.Q. Xu, Saturated Boundary Feedback Stabilization of a Linear Wave Equation, vol. 57, 2019, pp. 290–309, https://doi.org/10.1137/15M1034350.
[7] K. Braun, A. Pochert, M. Lindén, M. Davoudi, A. Schmidtchen, R. Nordström, M. Malmsten, Membrane interactions of mesoporous silica nanoparticles as carriers of antimicrobial peptides, J. Colloid Interface Sci. 475 (2016) 161–170, https://doi.org/10.1016/J.JCIS.2016.05.002.
[8] Y. Zhou, G. Quan, Q. Wu, X. Zhang, B. Niu, B. Wu, Y. Huang, X. Pan, C. Wu, Mesoporous silica nanoparticles for drug and gene delivery, Acta Pharm. Sin. B 8 (2018) 165–177, https://doi.org/10.1016/J.APSB.2018.01.007.
[9] K. Gou, X. Guo, Y. Wang, Y. Wang, Z. Sang, S. Ma, Y. Guo, L. Xie, S. Li, H. Li, Chiral microenvironment-responsive mesoporous silica nanoparticles for delivering indometacin with chiral recognition function, Mater. Des. 214 (2022), https://doi.org/10.1016/J.MATDES.2021.110359.
[10] N. Fan, R. Liu, P. Ma, X. Wang, C. Li, J. Li, Colloids and Surfaces B : Biointerfaces the On-O ff chiral mesoporous silica nanoparticles for delivering achiral drug in chiral environment, Colloids Surf. B Biointerfaces 176 (2019) 122–129, https://doi.org/10.1016/j.colsurfb.2018.12.065.
[11] B. Hu, J. Wang, Superiority of L-Tartaric Acid Modi Fi Ed Chiral Mesoporous Silica Nanoparticle as a Drug Carrier : Structure , Wettability , Degradation , Bio-Adhesion and Biocompatibility, 2020.
[12] H.U. Zaman, M.D.H. Beg, Preparation, structure, and properties of the coir fiber/polypropylene composites, J. Compos. Mater. 48 (2014) 3293–3301, https://doi.org/10.1177/0021998313508996.
[13] M.F. Anuar, Y.W. Fen, R. Emilia, M. Khaidir, Results in Physics Synthesis and Structural Properties of Coconut Husk as Potential Silica Source, vol. 11, 2018, pp. 1–4, https://doi.org/10.1016/j.rinp.2018.08.018.
[14] K. Dlomo, S.M. Mohomane, T.E. Motaung, Influence OF silica nanoparticles ON the properties OF cellulose COMPOSITE MEMBRANES: a current review, CELLULOSE CHEMISTRY AND TECHNOLOGY Cellulose Chem. Technol. 54 (2020) 765–775.
[15] I. Made Joni, Rukiah, C. Panatarani, Synthesis of silica particles by precipitation method of sodium silicate: effect of temperature, pH and mixing technique, AIP Conf. Proc. 2219 (2020) 80018, https://doi.org/10.1063/5.0003074/FORMAT/PDF.
[16] S. Sankar, N. Kaur, S. Lee, D.Y. Kim, Rapid sonochemical synthesis of spherical silica nanoparticles derived from brown rice husk, Ceram. Int. 44 (2018) 8720–8724, https://doi.org/10.1016/J.CERAMINT.2018.02.090.
[17] F. Pena-Pereira, R.M.B.O. Duarte, A.C. Duarte, Immobilization strategies and analytical applications for metallic and metal-oxide nanomaterials on surfaces, TrAC, Trends Anal. Chem. 40 (2012) 90–105, https://doi.org/10.1016/J.TRAC.2012.07.015.
[18] P. Paik, A. Gedanken, Y. Mastai, Enantioselective separation using chiral mesoporous spherical silica prepared by templating of chiral block copolymers, ACS Appl. Mater. Interfaces 1 (2009) 1834–1842, https://doi.org/10.1021/am9003842.
[19] B. Han, L. Shi, X. Gao, J. Guo, K. Hou, Y. Zheng, Z. Tang, Ultra-stable silica-coated chiral Au-nanorod assemblies: core–shell nanostructures with enhanced chiroptical properties, Nano Res. 9 (2016) 451–457, https://doi.org/10.1007/s12274-015-0926-4.
[20] K. Gou, Y. Wang, L. Xie, X. Guo, Y. Guo, J. Ke, L. Wu, S. Li, H. Li, Synthesis , structural properties , biosafety and applications of chiral mesoporous silica nanostructures, Chem. Eng. J. 421 (2021) 127862, https://doi.org/10.1016/j.cej.2020.127862.
[21] M. Cui, W. Zhang, L. Xie, L. Chen, L. Xu, Chiral mesoporous silica materials: a review on synthetic strategies and applications, Molecules 25 (2020) 3899, https://doi.org/10.3390/MOLECULES25173899, 25 (2020) 3899.
[22] M. Chekini, L. Guénée, V. Marchionni, M. Sharma, T. Bürgi, Twisted and tubular silica structures by anionic surfactant fibers encapsulation, J. Colloid Interface Sci. 477 (2016) 166–175, https://doi.org/10.1016/j.jcis.2016.05.049.
[23] X. Zhu, P. Duan, L. Zhang, M. Liu, Regulation of the chiral twist and supramolecular chirality in co-assemblies of amphiphilic L-glutamic acid with bipyridines, Chem. Eur J. 17 (2011) 3429–3437, https://doi.org/10.1002/CHEM.201002595.
[24] E. Gayathiri, P. Prakash, N. Karmegam, S. Varjani, M.K. Awasthi, B. Ravindran, Biosurfactants: potential and Eco-Friendly material for sustainable Agriculture and environmental safety—a review, Agronomy 12 (2022), https://doi.org/10.3390/agronomy12030662.
[25] M.C. Shutter, H. Akhondi, Tetracycline, Kucers the Use of Antibiotics: A Clinical Review of Antibacterial, Antifungal, Antiparasitic, and Antiviral Drugs, seventh ed., 2022, pp. 1195–1203, https://doi.org/10.1201/9781315152110.
[26] N. Saito, N. Takamura, G.P. Retuerma, C.H. Frayco, P.S. Solano, C.D. Ubas, A. V. Lintag, M.R. Ribo, R.M. Solante, A.Q. Dimapilis, E.O. Telan, W.S. Go, M. Suzuki, K. Ariyoshi, C.M. Parry, Frequent Community Use of antibiotics among a low-Economic Status Population in Manila, the Philippines: a Prospective Assessment using a Urine antibiotic Bioassay, Am. J. Trop. Med. Hyg. 98 (2018) 1512–1519, https://doi.org/10.4269/AJTMH.17-0564.
[27] V.K. Dik, M.G.H. van Oijen, H.M. Smeets, P.D. Siersema, Frequent Use of antibiotics is Associated with Colorectal Cancer Risk: results of a Nested Case–Control study, Dig. Dis. Sci. 61 (2016) 255, https://doi.org/10.1007/S10620-015-3828-0.
[28] H. Kaur, G.C. Mohanta, V. Gupta, D. Kukkar, S. Tyagi, Synthesis and characterization of ZIF-8 nanoparticles for controlled release of 6-mercaptopurine drug, J. Drug Deliv. Sci. Technol. 41 (2017) 106–112, https://doi.org/10.1016/J.JDDST.2017.07.004.
[29] M.X. Wu, Y.W. Yang, Metal–organic Framework (MOF)-Based drug/Cargo delivery and Cancer Therapy, Adv. Mater. 29 (2017), https://doi.org/10.1002/adma.201606134.
[30] S.K. Das, M.K. Bhunia, D. Chakraborty, A.R. Khuda-Bukhsh, A. Bhaumik, Hollow spherical mesoporous phosphosilicate nanoparticles as a delivery vehicle for an antibiotic drug, Chem. Commun. 48 (2012) 2891–2893, https://doi.org/10.1039/c2cc17181c.
[31] C.X. (Cynthia) Lin, S.Z. Qiao, C.Z. Yu, S. Ismadji, G.Q. (Max) Lu, Periodic mesoporous silica and organosilica with controlled morphologies as carriers for drug release, Microporous Mesoporous Mater. 117 (2009) 213–219, https://doi.org/10.1016/j.micromeso.2008.06.023.
[32] M. Takehara, I. Yoshimura, K. Takizawa, R. Yoshida, Surface active N-acylglutamate: I. Preparation of long chain N-acylglutamic acid, J. Am. Oil Chem. Soc. 49 (1972) 157–161, https://doi.org/10.1007/BF02633785.

[33] C. Huo, J. Ouyang, H. Yang, CuO nanoparticles encapsulated inside Al-MCM-41 mesoporous materials via direct synthetic route, Sci. Rep. 4 (2015), https://doi.org/10.1038/srep03682.
[34] N. Noor Aien Mohamed Abdul Ghani, M. Alam Saeed, I. Hazwani Hashim, Thermoluminescence (TL) Response of Silica Nanoparticles Subjected to 50 Gy Gamma Irradiation, 2017.
[35] M.A. Surma, A. Szczepaniak, J. Króliczewski, Comparative studies on detergent-assisted apocytochrome b6 reconstitution into liposomal bilayers monitored by zetasizer instruments, PLoS One 9 (2014), https://doi.org/10.1371/journal.pone.0111341.
[36] M. Thommes, K. Kaneko, A. V Neimark, J.P. Olivier, F. Rodriguez-reinoso, J. Rouquerol, K.S.W. Sing, Physisorption of Gases , with Special Reference to the Evaluation of Surface Area and Pore Size Distribution (IUPAC Technical Report), 2015, https://doi.org/10.1515/pac-2014-1117.
[37] H.M. Jang, E. Kan, Engineered biochar from agricultural waste for removal of tetracycline in water, Bioresour. Technol. 284 (2019) 437–447, https://doi.org/10.1016/j.biortech.2019.03.131.
[38] M.S. Manzar, T. Ahmad, M. Zubair, N. Ullah, H.A. Alqahtani, B.M.V. da Gama, J. Georgin, M. Nasir, N.D. Mu'azu, J.M. Al Ghamdi, H.A. Aziz, L. Meili, Comparative adsorption of tetracycline onto unmodified and NaOH-modified silicomanganese fumes: kinetic and process modeling, Chem. Eng. Res. Des. 192 (2023) 521–533, https://doi.org/10.1016/j.cherd.2023.02.047.
[39] Z. Li, L. Schulz, C. Ackley, N. Fenske, Adsorption of tetracycline on kaolinite with pH-dependent surface charges, J. Colloid Interface Sci. 351 (2010) 254–260, https://doi.org/10.1016/j.jcis.2010.07.034.
[40] Y.U.J. Wang, D.E.A.N. Jia, S.U.N. Rui-Juan, Z.H.U. Hao-Wen, D.M. Zhou, Adsorption and cosorption of tetracycline and copper(ll) on montmorillonite as affected by solution pH, Environ. Sci. Technol. 42 (2008) 3254–3259, https://doi.org/10.1021/es702641a.
[41] R.A. Figueroa, A. Leonard, A.A. Mackay, Modeling tetracycline antibiotic sorption to Clays, Environ. Sci. Technol. 38 (2003) 476–483, https://doi.org/10.1021/ES0342087.
[42] I. Turku, T. Sainio, E. Paatero, Thermodynamics of tetracycline adsorption on silica, Environ. Chem. Lett. 5 (2007) 225–228, https://doi.org/10.1007/S10311-007-0106-1/METRICS.
[43] M.S. Manzar, T. Ahmad, M. Zubair, N. Ullah, H.A. Alqahtani, B.M.V. da Gama, J. Georgin, M. Nasir, N.D. Mu'azu, J.M. Al Ghamdi, H.A. Aziz, L. Meili, Comparative adsorption of tetracycline onto unmodified and NaOH-modified silicomanganese fumes: kinetic and process modeling, Chem. Eng. Res. Des. 192 (2023) 521–533, https://doi.org/10.1016/J.CHERD.2023.02.047.
[44] D.K. Mahmoud, M.A.M. Salleh, W.A.W.A. Karim, A. Idris, Z.Z. Abidin, Batch adsorption of basic dye using acid treated kenaf fibre char: equilibrium, kinetic and thermodynamic studies, Chem. Eng. J. 181–182 (2012) 449–457, https://doi.org/10.1016/j.cej.2011.11.116.
[45] J. Zhou, F. Ma, H. Guo, Adsorption behavior of tetracycline from aqueous solution on ferroferric oxide nanoparticles assisted powdered activated carbon, Chem. Eng. J. 384 (2020), https://doi.org/10.1016/j.cej.2019.123290.
[46] Y. Peng, M. Azeem, R. Li, L. Xing, Y. Li, Y. Zhang, Z. Guo, Q. Wang, H. Hao Ngo, G. Qu, Z. Zhang, Zirconium hydroxide nanoparticle encapsulated magnetic biochar composite derived from rice residue: Application for As(III) and As(V) polluted water purification, J. Hazard Mater. 423 (2022) 127081, https://doi.org/10.1016/j.jhazmat.2021.127081.
[47] A.T. Ojedokun, O.S. Bello, Kinetic modeling of liquid-phase adsorption of Congo red dye using guava leaf-based activated carbon, Appl. Water Sci. 7 (2017) 1965–1977, https://doi.org/10.1007/s13201-015-0375-y.
[48] A. Pholosi, E.B. Naidoo, A.E. Ofomaja, Intraparticle diffusion of Cr(VI) through biomass and magnetite coated biomass: a comparative kinetic and diffusion study, S. Afr. J. Chem. Eng. 32 (2020) 39–55, https://doi.org/10.1016/j.sajce.2020.01.005.
[49] H.K. Boparai, M. Joseph, D.M. O'Carroll, Kinetics and thermodynamics of cadmium ion removal by adsorption onto nano zerovalent iron particles, J. Hazard Mater. 186 (2011) 458–465, https://doi.org/10.1016/J.JHAZMAT.2010.11.029.
[50] P.T.H. Hanh, K. Phoungthong, S. Chantrapromma, P. Choto, C. Thanomsilp, P. Siriwat, N. Wisittipanit, T. Suwunwong, Adsorption of tetracycline by magnetic mesoporous silica derived from bottom ash—biomass power plant, Sustainability 15 (2023) 4727, https://doi.org/10.3390/su15064727.
[51] M. Brigante, M. Avena, Biotemplated synthesis of mesoporous silica for doxycycline removal. Effect of pH, temperature, ionic strength and Ca2+ concentration on the adsorption behaviour, Microporous Mesoporous Mater. 225 (2016) 534–542, https://doi.org/10.1016/j.micromeso.2016.01.035.
[52] C.H. Giles, T.H. MacEwan, S.N. Nakhwa, D. Smith, Studies in adsorption. Part XI.* A system, J. Chem. Soc. 846 (1960) 3973–3993.
[53] A. Dąbrowski, P. Podkościelny, Z. Hubicki, M. Barczak, Adsorption of phenolic compounds by activated carbon - a critical review, Chemosphere 58 (2005) 1049–1070, https://doi.org/10.1016/j.chemosphere.2004.09.067.
[54] A. Günay, E. Arslankaya, I. Tosun, Lead removal from aqueous solution by natural and pretreated clinoptilolite: adsorption equilibrium and kinetics, J. Hazard Mater. 146 (2007) 362–371, https://doi.org/10.1016/J.JHAZMAT.2006.12.034.
[55] R. Rusmin, B. Sarkar, Y. Liu, S. McClure, R. Naidu, Structural evolution of chitosan–palygorskite composites and removal of aqueous lead by composite beads, Appl. Surf. Sci. 353 (2015) 363–375, https://doi.org/10.1016/J.APSUSC.2015.06.124.
[56] B. Van der Bruggen, Freundlich Isotherm, Encyclopedia of Membranes, 2016, pp. 834–835, https://doi.org/10.1007/978-3-662-44324-8_254.
[57] A.A.A. Darwish, M. Rashad, H.A. AL-Aoh, Methyl orange adsorption comparison on nanoparticles: isotherm, kinetics, and thermodynamic studies, Dyes Pigments 160 (2019) 563–571, https://doi.org/10.1016/j.dyepig.2018.08.045.
[58] M.L. Bruschi, Mathematical models of drug release, in: Strategies to Modify the Drug Release from Pharmaceutical Systems, Elsevier, 2015, pp. 63–86, https://doi.org/10.1016/b978-0-08-100092-2.00005-9.

Twisted-chiral mesoporous silica from coconut husk waste designed for high-performance drug uptake and sustained release

ORIGINALITY REPORT

3%	3%	3%	2%
SIMILARITY INDEX	INTERNET SOURCES	PUBLICATIONS	STUDENT PAPERS

PRIMARY SOURCES

1	Noerma J. Azhari, Bahaul F. Al-Haq, A.C. S Axel, Muhammad A. Rifialdy et al. "Ethylene-to-Aromatics over Metal-Free Hierarchical MFI Zeolite: Boosting the BTX Yield", Results in Engineering, 2025 Publication	1%
2	www.um.edu.mt Internet Source	1%
3	Guixiao Ji, Yinfeng Han, Jiajia Wang, Junshan Sun, Xianqiang Huang, Chang'an Wang. "A 3D Zn-MOF for Luminescent Sensing of p-Nitrophenol and L-Lysine, and Enhanced Proton Conduction Properties", Dyes and Pigments, 2024 Publication	1%
4	Tammy Laysandra, Felycia Edi Soetaredjo, Jindrayani Nyoo Putro, Jenni Lie et al. "Study of pharmaceutical contaminant adsorption using HKUST-1 as metal-organic framework	1%

model", Environmental Nanotechnology, Monitoring & Management, 2023

Publication

Exclude quotes	On	Exclude matches	< 1%
Exclude bibliography	On		